JOURNAL OF Materials CHEMISTRY

Syntheses, powder neutron diffraction structures and Mössbauer studies of some complex iron oxyfluorides: $Sr_3Fe_2O_6F_{0.87}$, Sr_2FeO_3F and $Ba_2InFeO_5F_{0.68}$

G. Simon Case,[a] Andrew L. Hector,[b] William Levason,[b] Richard L. Needs,[b] Michael F. Thomas[a] and Mark T. Weller*[b]

[a]*Department of Physics, Oliver Lodge Laboratory, Oxford Street, Liverpool, UK L69 7ZF*
[b]*Department of Chemistry, University of Southampton, Highfield, Southampton, UK SO17 1BJ. E-mail: mtw@soton.ac.uk*

Received 15th July 1999, Accepted 16th August 1999

Sr_2FeO_3F and the novel phases $Sr_3Fe_2O_6F_{0.87}$ and $Ba_2InFeO_5F_{0.68}$ have been prepared and their structures investigated by powder neutron diffraction methods. Sr_2FeO_3F crystallises with the T* modification of the K_2NiF_4 structure owing to oxide/fluoride ordering. $Sr_3Fe_2O_6F_{0.87}$ and $Ba_2InFeO_5F_{0.68}$ are mixed valent phases prepared by reaction of anion deficient iron(III) materials with gaseous fluorine. $Sr_3Fe_2O_6F_{0.87}$ is a Ruddlesden–Popper type material which has been shown by Mössbauer spectroscopy to contain iron(III) and iron(V). $Ba_2InFeO_5F_{0.68}$ is the first example of an iron oxyfluoride with a perovskite-type structure.

Introduction

Interest in layered oxyfluorides stems from the structural, valence and compositional changes, compared with simple oxides or fluorides, which are observed with the simultaneous presence of these two ions in a material. Oxide and fluoride ions are very similar in size but have different oxidation states, so can often stabilise the same structures for different cation oxidation states. An example of structural modification in this manner is the fluorination of Sr_2CuO_3, which affords the 46 K superconductor $Sr_2CuO_2F_{2+\delta}$.[1] Here the fluoride ions solely occupy the apical sites of the copper, resulting in effective CuO_2 square planes and an interstitial fluoride site in the newly formed SrF rocksalt layer.

The synthesis of complex oxides of iron-(IV) and -(V) generally requires highly oxidising conditions. Partial oxidation can often be achieved under flowing oxygen at ambient pressures but full oxidation usually requires reaction in high pressures of oxygen. For example in the perovskite system, $SrFeO_{3-x}$ may be synthesised under oxygen at ambient pressure, whereas $SrFeO_3$ must be prepared under several hundred atmospheres of oxygen.[2] $SrFeO_3$ has been shown, by Mössbauer spectroscopy, to contain only iron(IV).[3] Substitution of strontium for calcium[4] or lanthanum,[5] even at low levels, results in a disproportionation to iron(III) and iron(V).

Oxides exhibiting the K_2NiF_4 structure, and structures related to it, have been the subject of intense research activity propelled by the discovery in 1986 of superconductivity in the series $La_{2-x}Ba_xCuO_4$, the first high temperature superconductors.[6] A doubling of the perovskite layer leads to a set of compounds in the series first described by Ruddlesden and Popper[7] in 1957 (where K_2NiF_4 is the first member), with stoichiometry $AO(ABO_3)_2$. The fully oxidised strontium iron phases with these two structures are Sr_2FeO_4[8] and $Sr_3Fe_2O_7$.[9] Mössbauer data have shown that Sr_2FeO_4 contains iron(IV), which orders with at least four magnetically different iron(IV) sites below T_N (60 K).[10] The Mössbauer behaviour of $Sr_3Fe_2O_7$ is very similar to that observed for $CaFeO_3$; two components of equal intensity are observed, corresponding to Fe^{3+} and Fe^{5+}, which become two magnetic sextet components below T_N (110 K).[10]

There are only a limited number of reports of oxyfluorides with perovskite and Ruddlesden–Popper type structures. The known examples of perovskite oxyfluorides are $BaScO_2F$,[11] $ANbO_2F$ (A = Na, K and Rb),[12] $KTiO_2F$[13] and Tl_2O_2F (which contains Tl^+ and Tl^{3+} on the A and B sites respectively).[14] The latter two phases only form at very high pressure. A number of related bronze, cryolite and elpasolite phases have also been reported.[15] The K_2NiF_4-type examples are Ba_2MO_3F (M = In, Sc),[16] $Sr_2CuO_2F_{2+\delta}$,[1] K_2NbO_3F,[17] $Sr_2FeO_{4-x}F_x$ $(0.8 < x < 1)$[18] and $Ca_2MnO_{4-x}F_x$ $(x < 0.3)$.[19] The indium phase has been shown to contain ordered oxide/fluoride sites resulting in effective square pyramidal InO_5 coordination to the B-cation, whereas the scandium phase has disordered oxygen/fluorine mixing at the apical position.[16] In $Sr_2CuO_2F_{2+\delta}$ cation ordering leads to sheets of CuO_2 square planes.[1] $Ba_3In_2O_5F_2$ also has segregation of fluoride and oxide, the structure can be considered as vertex sharing indium–oxygen square pyramids separated by BaF layers.[20] Fluorination of $La_{1.9}Sr_{1.1}Cu_2O_6$ results in replacement of an oxide with two fluorides, the resulting stoichiometry is $La_{1.9}Sr_{1.1}Cu_2O_5F_{2.1}$, and the extra fluoride occupies an interstitial site.[21] $La_{1.2}Sr_{1.8}Mn_2O_7$ may be fluorinated with insertion of two fluorides into the interstitial site, the result is $La_{1.2}Sr_{1.8}Mn_2O_7F_2$.[21]

Here, the synthesis and structures of three oxyfluoride materials containing iron are reported. The mixed-valence $Sr_3Fe_2O_6F_x$ and $Ba_2InFeO_5F_x$ are new materials produced by fluorination of iron(III) oxides with defect structures. Sr_2FeO_3F is synthesised by a modified route and the structure investigated in detail and shown to contain ordered anions.

Experimental

Red–brown $Sr_3Fe_2O_6$ and Ba_2InFeO_5 were prepared by literature methods.[9,22] Samples were fluorinated in a 0.3 dm^3 Monel autoclave using gaseous fluorine or fluorine–nitrogen mixtures supplied from a metal vacuum line. The autoclave was heated with an external furnace and internal temperatures were not monitored. Products were apparently air stable, but were handled in a nitrogen-filled glove box to guard against possible slow hydrolysis.

$Sr_3Fe_2O_6$ was fluorinated under a variety of conditions. Use of low pressures of fluorine or fluorine/nitrogen mixtures

resulted in partially reacted samples or heavy contamination with SrF_2. A fairly short reaction time (2 h) with an excess of fluorine at *ca.* 140 °C yielded pure black samples but with poor crystallinity. The best samples for structural characterisation were produced by heating for longer periods of time, with a large excess of fluorine and careful temperature control. The 0.85 g sample used for characterisation purposes was produced at a temperature (external to the autoclave) of 120 °C, heated for 10 h with 2 atm of fluorine. If the temperature exceeds *ca.* 150 °C, even briefly, then a solid red lump of product is obtained which has been identified as a mixture of SrF_2 and $Sr_3Fe_5F_{19}$.[23] Below 120 °C the samples are only partially reacted.

Fluorination of Ba_2InFeO_5 was carried out on a 0.6 g sample at 300 °C for *ca.* 15 h, yielding black products. Lower temperatures or shorter reaction times resulted in incomplete reaction, whereas a higher temperature yielded products containing BaF_2.

Fluorination of $Sr_2Fe_2O_5$ (200 °C for 2 days, 2 atm F_2) resulted in two cubic perovskite phases. These had lattice parameters of 3.95 and 3.87 Å, and the phase fractions refined to a ratio of *ca.* 1 : 1. At lower temperatures (150 °C) little change in the starting material was observed. A shorter reaction time at 200 °C (5 h) resulted in a mixture of the 3.87 Å cubic perovskite and $Sr_2Fe_2O_5$. Higher temperatures (250 °C) resulted in a dark red amorphous material and SrF_2.

In the synthesis of Sr_2FeO_3F, high temperature synthesis from $SrCO_3$, SrF_2 and Fe_2O_3 in an inert atmosphere, as previously described,[18] always resulted in partially oxidised, black products ($Sr_2FeO_{3+x}F_{1-x}$). The requirements of gas stream purity were clearly not met by passing argon over glowing Fe wire. Successful synthesis was achieved by a cyclic process of heating for 24 h in argon at 900 °C, followed by heating for 24 h in a 5% H_2–N_2 mixture at 850 °C in a platinum foil boat. Three cycles of this procedure, with intermediate regrinding, yielded pure, polycrystalline, brick red samples.

Powder X-ray diffraction patterns were collected using a Siemens D5000 diffractometer employing Cu-Kα_1 radiation ($\lambda = 1.5406$ Å) with a step size of 0.02°. Time-of-flight PND data were collected for 4 h on the POLARIS medium resolution diffractometer at the Rutherford Appleton Laboratory. Data from the back-scattering detector bank were used for refinement. Full profile Rietveld analysis was carried out using the GSAS program suite.[24]

The Mössbauer spectra were obtained with a conventional transmission spectrometer using a double-ramp waveform to give a flat background. Absorbers were prepared of finely ground samples weighed to give optimum signal-to-noise[25] and mixed with boron nitride to randomise the orientation of the microcrystals. Sources of up to 100 mCi of ^{57}Co in Rh were used and the spectrometers were calibrated using α-iron at room temperature. Values of isomer shift are quoted with respect to α-iron at 300 K.

Samples of $Sr_3Fe_2O_6F_x$ and $Ba_2InFeO_5F_x$ were analysed for fluoride content colorimetrically by the lanthanum alizarin complexone method.[26] Samples were dissolved in a minimum quantity of concentrated HCl. The iron was found to interfere with the analysis and so was precipitated with KOH. After filtration, the sample was made up to a known volume and stored in a sealed polythene bottle until use. The alizarin dye was prepared as previously described.[26] 10 ml aliquots of fluoride solution, of varying concentration, were mixed with 15 ml of the dye solution and made up to 50 ml. After 20 min the UV–VIS spectrum was recorded in 1 cm glass cells using a Perkin Elmer Lambda 19 spectrometer in the range 1000–300 nm. The absorbance at 616.8 nm was measured and the fluoride content read from a calibration curve prepared using KF solutions. Fluoride content was plotted against the known mass of sample in the solution. Remaining iron was found to affect the measurement, resulting in a curved graph, but its effect was small at high fluoride concentration. Thus the plot was extrapolated from five measured points, as a second order polynomial, and the fluoride content of the sample was read at the maximum of this curve. Analysed percentage fluoride in $Sr_3Fe_2O_6F_x$: 3.3%; calculated for $Sr_3Fe_2O_6F$: 3.9%. Analysed percentage fluoride in $Ba_2InFeO_5F_x$: 2.7%; calculated for Ba_2InFeO_5F: 3.5%.

Energy dispersive X-ray analysis (EDX) was performed using a JEOL JSM-6400 scanning electron microscope in conjunction with a Tracor Series II EDX analysis system at Southampton Oceanography Centre. The ratio of cations always matched that expected to within experimental error. More importantly, no variations in morphology or composition were observed for any of the samples so indicating good homogeneity.

Structure refinements

$Sr_3Fe_2O_6F_x$

The product resulting from fluorination of $Sr_3Fe_2O_6$ was first investigated using PXD data. The data were modelled to the *I4/mmm* structure of $Sr_3Fe_2O_7$ and refined to a 3.87×20.75 Å cell. The *c*-axis is significantly longer than that of $Sr_3Fe_2O_7$ (20.15 Å) whilst the *a*-axis is quite similar (3.85 Å). In order to obtain accurate anion positions and occupation factors, powder neutron diffraction data were collected.

Since the scattering lengths of oxygen (5.80 fm) and fluorine (5.65 fm) are so similar,[27] no attempt was made to distinguish between them during refinement of the PND data (all anion sites were refined as oxygen). In common with the X-ray study, reflections were fairly broad. This is of little surprise since the synthesis temperature is so low, and broad reflections are common in oxyfluorides synthesised in this way (for example $Sr_2CuO_2F_{2+\delta}$[1]).

Initially the lattice parameters, zero point, background and peak shape were refined. Further parameters were cation and anion positions and isotropic temperature factors. It was found to be necessary to constrain together the temperature factors of the anion sites to increase the stability of refinement of these parameters, though later in the refinement it was found to be possible to remove the constraint on the equatorial site. It was also necessary to allow preferred orientation to refine to a fairly large value in the 001 direction. Finally the fractional occupancies of the apical anion sites were refined. Extra reflections were identified as vanadium from the neutron sample can and these were modelled in the refinement. Weak reflections due to an impurity phase remain unidentified and were excluded from the refinement (2.883, 2.448, 2.178, 2.036, 1.444 and 1.027 Å). The final refined positional parameters obtained are listed in Table 1 and the final fit is given in Fig. 1.

Sr_2FeO_3F

Powder X-ray diffraction patterns of Sr_2FeO_3F showed a slightly larger unit cell than partially oxidised ($Sr_2FeO_{3+x}F_{1-x}$) samples, in agreement with Menil *et al.*[18] and consistent with the presence of only Fe^{3+}. Initial investigations of the structure

Table 1 Refined positional parameters for $Sr_3Fe_2O_6F_x$[a]

Atom	Site	*x*	*y*	*z*	B_{iso}/Å^2	Occupancy
Sr	2b	0	0	1/2	1.78(15)	1
Sr	4e	0	0	0.31517(25)	0.12(5)	1
Fe	4e	0	0	0.09116(31)	1.64(6)	1
O	8g	0	1/2	0.09736(33)	1.06(6)	1
O	4e	0	0	0.1998(9)	3.15(20)	0.93(3)
O	2a	0	0	0	3.15(20)	0.94(5)

[a]Space group *I4/mmm*, $a = 3.8664(12)$ Å, $c = 20.7794(30)$ Å, $R_{wp} = 5.56\%$, $R_p = 5.86\%$.

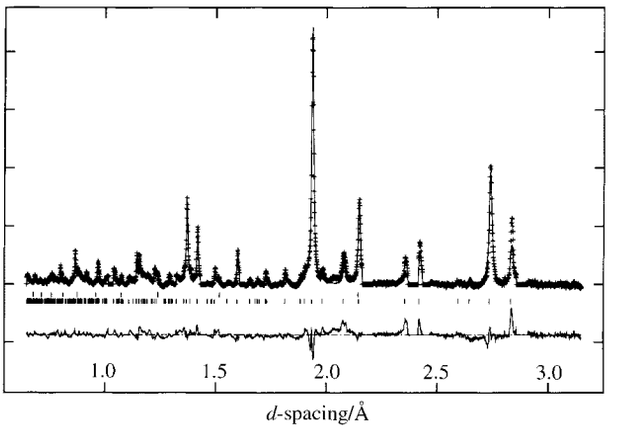

Fig. 1 Fit to the PND pattern of $Sr_3Fe_2O_6F_x$. Data points are marked as crosses, profile fit as the upper continuous line and difference as the lower continuous line. The lower set of tick marks represents the $Sr_3Fe_2O_6F_x$ reflection positions, the upper set those of vanadium.

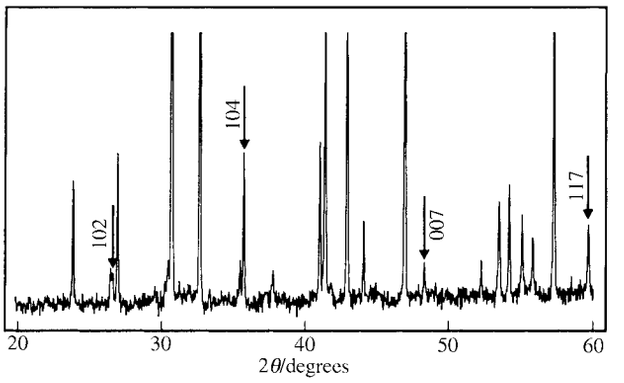

Fig. 2 The PXD pattern of Sr_2FeO_3F, showing the peaks which can only be assigned using a primitive cell.

using the model proposed by Galasso and Derby,[28] with a disordered mixture of oxygen and fluorine on the apical iron sites, were unsuccessful with some small peaks in the diffraction pattern unindexed. This model uses the normal body centred T structure,[29] in the space group *I*4/*mmm*. Closer inspection of the diffraction pattern showed superstructure reflections similar to those observed for Ba_2InO_3F,[16] Fig. 2, corresponding to a primitive tetragonal cell. Using as a model the *P*4/*nmm* T*-type structure[29] of Ba_2InO_3F, the structure was successfully refined. This model results, in Ba_2InO_3F, in the apical sites occupied alternately by oxide and fluoride.

High errors on the anion positions derived from PXD data precluded their use in assignment of oxide and fluoride positions, so PND data were collected to overcome this problem.

Inspection of the Sr_2FeO_3F data after the refinement of lattice parameters and zero point showed there to be a few unindexed peaks at large *d* spacings. The magnetic ordering temperature of Sr_2FeO_3F has been reported as 358 K by Menil *et al.*[18] from Mössbauer data. The PND data collection temperature of 298 K is sufficiently below this value as to lead to the expectation of the observation of peaks arising from the magnetic cell. This supposition is further supported by the saw-tooth shape of these peaks arising from two-dimensional magnetic ordering, characteristic of a metal contained in a K_2NiF_4 type structure. Attempts to index these reflections were partially successful on a $\sqrt{2}a \times \sqrt{2}a \times c$ cell, however, owing to the low intensity and limited number of peaks it is impossible to determine the cell unequivocally. The angular ranges containing these peaks were therefore excluded from the refinement (1.981–2.081, 2.126–2.157, 2.251–2.306, 2.344–2.479, 2.564–2.701, 2.769–2.874 Å). The refinement converged smoothly with the inclusion of anisotropic thermal parameters on all sites. The final positional parameters are listed in Table 2.

$Ba_2InFeO_5F_x$

The product of fluorination of Ba_2InFeO_5 is a simple defect cubic perovskite and PXD data indicated a lattice parameter of 4.16 Å. PND data were used to obtain the fractional occupation of the anion position through refinement of the site occupancy factor of a mixed anion site. Oxygen was fixed at 5/6 occupation and the fluorine fraction was refined. The procedure was similar to that used for $Sr_3Fe_2O_6F_x$ and the positional parameters are listed in Table 3.

Mössbauer spectroscopy studies

The Mössbauer spectrum of Sr_2FeO_3F has been investigated previously[18] and shown to contain only distorted octahedral iron(III) sites, as also indicated by the brick red colour. The variable temperature data obtained in this work demonstrate a charge state of Fe^{3+} from 4.2 to 390 K. These data will be published elsewhere with the data for the isomorphous chloride and bromide systems.[30] The ^{57}Fe Mössbauer spectra of the

Table 2 Refined positional parameters for Sr_2FeO_3F[a]

Atom	Site	*x*	*y*	*z*	B_{11}/Å^2	B_{22}/Å^2	B_{33}/Å^2
Sr1	2c	1/4	1/4	0.37773(7)	0.76(3)	0.76(3)	0.54(3)
Sr2	2c	1/4	1/4	0.10471(7)	0.74(3)	0.74(3)	0.47(3)
Fe	2c	3/4	3/4	0.22751(5)	0.41(1)	0.41(1)	0.72(3)
O1	2c	3/4	3/4	0.08290(9)	1.28(3)	1.28(3)	0.32(5)
O2	4f	3/4	1/4	0.253&0(6)	0.79(3)	0.37(2)	1.06(4)
F	2c	3/4	3/4	0.4348(1)	2.94(5)	2.94(5)	1.07(6)

[a]Space group *P*4/*nmm*, $a = 3.8660(5)$ Å, $c = 13.1724(2)$ Å, $R_{wp} = 2.20\%$, $R_p = 2.55\%$.

Table 3 Refined positional parameters for $Ba_2InFeO_5F_x$

Atom	Site	*x*	*y*	*z*	B_{iso}/Å^2	Occupancy
Ba	1b	1/2	1/2	1/2	1.57(5)	1
In	1a	0	0	0	3.19(5)	1/2
Fe	1a	0	0	0	3.19(5)	1/2
O	3d	0	0	1/2	2.33(3)	0.833
F	3d	0	0	1/2	2.33(3)	1.106(7)

[a]Space group *Pm*3*m*, $a = 4.16440(13)$ Å, $R_{wp} = 1.84\%$, $R_p = 2.79\%$.

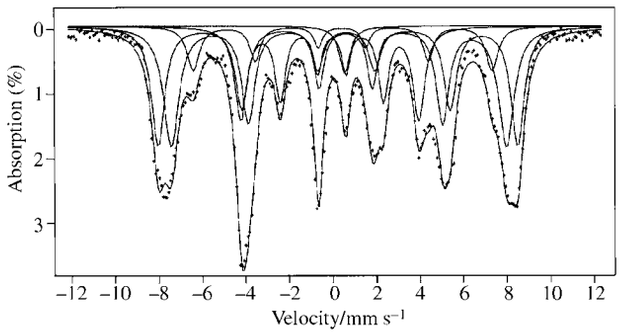

Fig. 3 Mössbauer spectrum of $Sr_3Fe_2O_6F_x$ at 4.2 K.

mixed valence compounds $Sr_3Fe_2O_6F_x$ and $Ba_2InFeO_5F_x$ were also collected to ascertain the iron oxidation states.

The 4.2 K spectrum of $Sr_3Fe_2O_6F_x$ is qualitatively very similar to that of $Sr_3Fe_2O_7$.[10] A good fit was obtained with four magnetic sextet components as listed in Table 4 and shown in Fig. 3. In fitting to spectra of powder samples with random orientation of sample microcrystals the areas of the outer : middle : inner doublets composing the magnetic sextet are fixed to the theoretical ratios of 3 : 2 : 1. Three sextets have similar isomer shifts (IS) and hyperfine fields (H_i), centred around 0.44 mm s^{-1} and 470 kG, respectively, and these are assigned as iron(III). The fitting parameters for these sextets agree well with the 50% iron(III) sextet observed for $Sr_3Fe_2O_7$ [IS = 0.32 mm s^{-1}, H_i = 417 kG, quadrupole shift (QS) = −0.07 mm s^{-1}). The fourth sextet, representing 22% of the total peak area, has a very different isomer shift. Its value is similar to that observed for the iron(V) component of $Sr_3Fe_2O_7$ (with an isomer shift of −0.06 mm s^{-1}). The fit gave a very small quadrupole interaction value for this sextet, which is consistent with Fe^{5+} ($3d^3$) rather than the Jahn–Teller ion Fe^{4+} ($3d^4$) which would be expected to distort its site.

At 300 K, the Mössbauer spectrum of $Sr_3Fe_2O_6F_x$ also bears resemblance to that of $Sr_3Fe_2O_7$.[10] A good fit to the data was obtained using a doublet and a singlet, Fig. 4 and Table 4. The doublet, with an isomer shift of 0.38 mm s^{-1}, is assigned as iron(III). The singlet is assigned as iron(V) since no quadrupole interaction is observed, which would be expected for iron(IV), and the isomer shift is very negative.

The Mössbauer spectra at 300 and 4.2 K are consistent in providing evidence for mixed iron(III)/iron(V) composition in $Sr_3Fe_2O_6F_x$. The proportion of iron(V) is seen to be 22 ± 2% from the 4.2 K spectrum and 27 ± 4% from the 300 K spectrum. These values are consistent within experimental errors but the 4.2 K value is seen as more reliable since the absorption peak in the spectrum at *ca.* −2.5 mm s^{-1}, characteristic of the iron(V) component, allows this component to be scaled more sensitively than is the case for the singlet component in the 300 K spectrum which is not resolved. The change in the value of the isomer shift between 4.2 and 300 K is qualitatively accounted for by the second order Doppler shift.

^{57}Fe Mössbauer spectra of $Ba_2InFeO_5F_x$ were more difficult to obtain owing to the smaller iron content and heavy atomic absorption from barium and indium. The spectrum at 300 K was fitted with an Fe^{3+} doublet and a singlet, fitting parameters are listed in Table 5 and the spectrum is shown in Fig. 5. The singlet is difficult to assign. The lack of quadrupolar interaction indicates iron(V) but the value of the isomer shift lies between the value observed for iron(V) in $Sr_3Fe_2O_6F_x$ and the iron(III) values. The isomer shift is, however, similar to that observed for iron(V) in $Sr_3Fe_2O_7$.[10] The 4.2 K spectrum was found to be very broad and weak. This may be attributed to the magnetic ordering and to a spread of hyperfine fields resulting from the range of iron environments. When fitted with two sextet components the isomer shifts are consistent with iron(III) and a more highly oxidised iron component. This component does not indicate

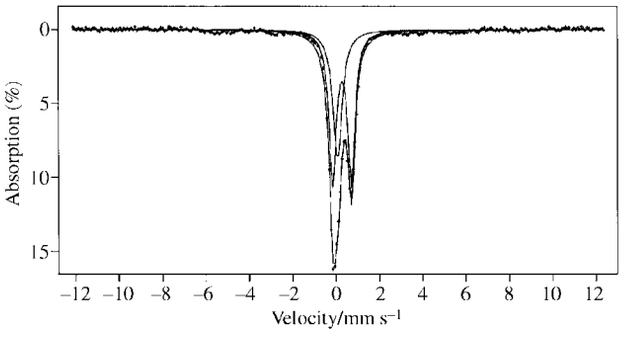

Fig. 4 Mössbauer spectrum of $Sr_3Fe_2O_6F_x$ at 300 K.

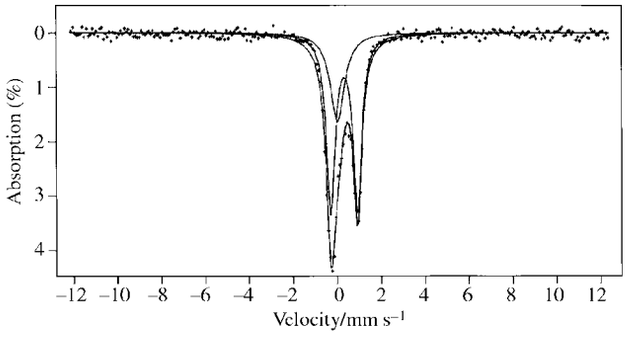

Fig. 5 Mössbauer spectrum of $Ba_2InFeO_5F_x$ at 300 K.

Table 4 Mössbauer parameters for $Sr_3Fe_2O_6F_x$

T/K	χ^2 (%)	Feature	IS/mm s^{-1}	QS/mm s^{-1}	H_i/kG	Width/mm s^{-1}	Normalised area
4.2	3.00	Sextet	0.43(3)	−0.38(2)	512(2)	0.70(4)	0.32(2)
		Sextet	0.44(3)	−0.31(2)	477(2)	0.70(4)	0.35(2)
		Sextet	0.47(3)	0.04(2)	425(2)	0.57(4)	0.11(2)
		Sextet	−0.07(2)	−0.09(2)	253(2)	0.61(4)	0.22(2)
300	1.93	Doublet	0.38(2)	−0.64(2)		0.47(2)	0.73(4)
		Singlet	−0.17(2)			0.32(2)	0.27(4)

Table 5 Mössbauer parameters for $Ba_2InFeO_5F_x$

T/K	χ^2 (%)	Feature	IS/mm s^{-1}	QS/mm s^{-1}	H_i/kG	Width/mm s^{-1}	Normalised area
4.2	1.22	Sextet	0.49(4)	0.11(3)	386(5)	1.88(4)	0.70(4)
		Sextet	0.32(4)	0.00(2)	179(5)	1.88(4)	0.30(4)
300	1.55	Doublet	0.31(2)	1.22(3)		0.47(3)	0.70(4)
		Singlet	0.01(2)			0.77(4)	0.30(4)

Fe^{4+} or Fe^{5+} with any certainty because of the poor spectrum definition.

Bond-valence calculations

$Sr_3Fe_2O_6F_x$ and Sr_2FeO_3F have more than one possible anion distribution. Differentiation between oxide and fluoride sites cannot be achieved directly *via* diffraction methods owing to their near identical X-ray and neutron scattering abilities. The assignment of a particular site by bond-valence calculations has been shown to be effective with Ba_2MO_3F (M = In, Sc) and $Ba_3In_2O_5F_2$.[16,20]

Bond valence calculations were carried out using published parameters.[31a] The fluoride ions in $Sr_3Fe_2O_6F_x$ were considered only likely to reside on one of the two apical positions. The *a*-axis was similar to that found throughout the $Sr_3Fe_2O_x$ ($6 < x < 7$) system ($3.853 < a < 3.892$ Å),[9] so the equatorial anions were all assumed to be oxide. The results of bond valence calculations for the apical positions are shown in Table 6. The 2a site is at the centre of the double perovskite layer and is the vacant site in $Sr_3Fe_2O_6$. This site was expected to contain fluoride since it is vacant in the parent material, but the calculation clearly indicates oxide as the only good match. The 4e site, located in the rocksalt layer, is not oxide but is not a good match to fluoride alone and is believed to contain a mixture of both anion types. The iron valence is calculated as 3.451 or 3.382 with the 4e site assigned as oxide or fluoride, respectively.

Sr_2FeO_3F was expected to have the same oxide/fluoride ordering as is observed in Ba_2InO_3F since the same superstructure was used in refining the diffraction data for both phases. The results of the bond valence calculation are shown in Table 7. These values clearly support the ordered model.

The very weak iron–fluorine bond valence value in Sr_2FeO_3F (0.057) shows that iron is effectively in square pyramidal coordination to the five oxygens with fluorine effectively non-bonded to iron. In $Sr_3Fe_2O_6F_x$ the equivalent anion site, 4e, is occupied by a mixture of oxide and fluoride and is quite strongly bonded to iron.

Discussion

The product of fluorination of $Sr_3Fe_2O_6$ has anion site occupations, according to the PND refinements, resulting in a composition $Sr_3Fe_2X_{6.87}$. This composition was derived by refining all anion positions as oxide. A composition of $Sr_3Fe_2O_6F_{0.87}$ requires a fluoride content of 3.4% which is a good match to the analysed fluoride content of 3.3%. The iron oxidation state with this composition would be $Fe^{3.44+}$ which, if present as iron(III) and iron(V) as shown by the Mössbauer, would require 22% iron(V). These measurements are reasonably self consistent and this is believed to be a good estimate of the composition.

Table 6 Bond valence calculation for $Sr_3Fe_2O_6F_x$

Anion site	Bonds considered	Calculation as O	Calculation as F
4e	Sr–X 2.750 Å (×4)	0.725	0.587
	Sr–X 2.503 Å (×1)	0.353	0.286
	Fe–X 2.140 Å (×1)	0.357	0.288
	Anion valence:	1.435	1.16
2a	Sr–X 2.736 Å (×4)	0.753	0.610
	Fe–X 1.939 Å (×2)	1.230	0.990
	Anion valence:	1.960	1.600

Table 7 Calculated bond valences for Sr_2FeO_3F

Ion	O1	O2	F	Cation valence
Fe	0.675	2.300	0.057	3.031
Sr1		1.307	0.737	2.045
Sr2	1.109	0.717		1.826
Anion valence	1.783	2.162	0.794	

The quality of the powder neutron diffraction data is limited by the sample quality and it was necessary to tie together the apical anion site temperature factors in order to stabilise the refinement. Non-ideal diffraction data are common in fluorinated materials and low temperature preparations and the detailed structural information which has been extracted from such data should be regarded with some caution. A fairly large preferred orientation (using the March–Dollase model[31b] in the 001 direction with $R_0 = 1.50$) was also used in the refinement, this is interpreted as accounting for some reduction in crystallinity in the *z*-direction during fluorination.

The structure of $Sr_3Fe_2O_6F_{0.87}$ is shown in Fig. 6, with the structure of the parent material also shown for comparison. The lattice parameters of $Sr_3Fe_2O_{7-x}$ vary from 3.89–20.03 Å for $x = 0$ to 3.85–20.15 Å for $x = 1$. For $Sr_3Fe_2O_6F_{0.87}$ the *a* parameter (3.87 Å) is very similar to the oxides but the *c* parameter (20.78 Å) is considerably elongated. This reflects the location of the fluoride ions on an apical site. Disorder, from mixed anions and partial site occupations, also results in high temperature factors in the PND refinement for the apical anion sites and some instability in their refinement.

Fig. 6 clearly shows that the fluoride in $Sr_3Fe_2O_6F_{0.87}$ is not inserted into the expected site, which was vacant in $Sr_3Fe_2O_6$. An interesting point is that the analysis results indicate that no oxide is lost during this process. This makes it highly unlikely that the fluorination process involves oxide displacement *out* of the structure (by fluoride and from the rocksalt layer), followed by reinsertion of oxide into the vacant site. Thus some kind of rearrangement process is required. Only one of the iron sites in each pair may undergo such a rearrangement, as demonstrated in Fig. 6, since the vacant site is then occupied for the other iron. Alternatively, neighbouring pairs of iron sites could take

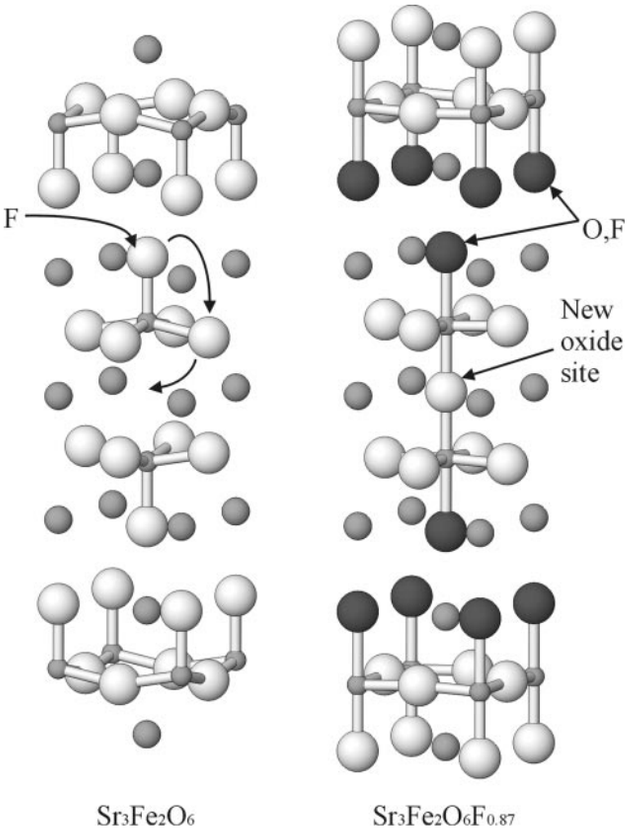

Fig. 6 Structures of $Sr_3Fe_2O_6$ and $Sr_3Fe_2O_6F_{0.87}$. Oxide ions shown in white, the mixed oxide/fluoride site in dark grey.

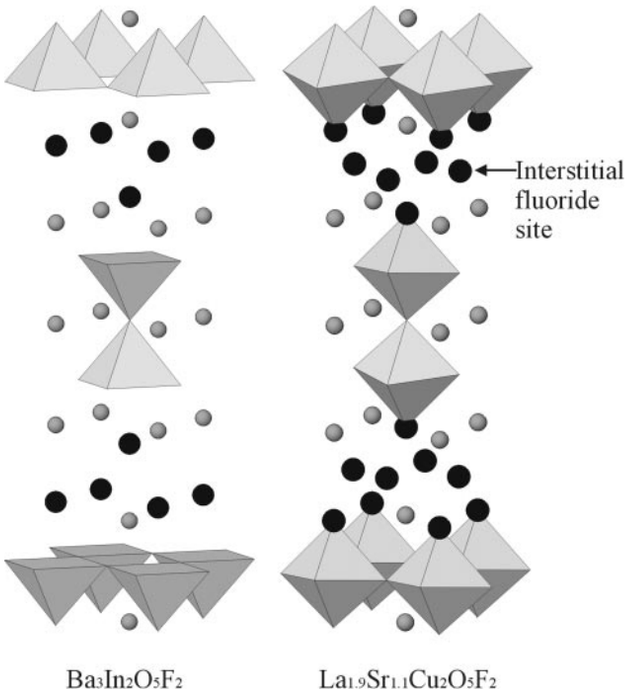

Fig. 7 Other Ruddlesden–Popper oxyfluorides. Large black spheres represent the fluoride sites.

oxygen, in which case both irons in a pair could coordinate fluorine.

The observation of sextet components in the Mössbauer spectrum at 4.2 K clearly shows that the phase is magnetically ordered. $Sr_3Fe_2O_7$ magnetically orders through neighbouring iron sites in the perovskite bilayer taking opposing spins (hence the ordering is two dimensional). This is the likely scenario here, though with the added complication of the disordered fluoride distribution, hence the four sextet components observed rather than the two observed with $Sr_3Fe_2O_7$. A low temperature neutron study might resolve this, although difficulties would probably be encountered with data quality.

Examples of $n=2$ Ruddlesden–Popper oxyfluorides which have been reported previously are shown in Fig. 7. $Ba_3In_2O_5F_2$ was synthesised by solid state methods using BaF_2 as a fluoride source.[16] $La_{1.9}Sr_{1.1}Cu_2O_5F_2$ was made by fluorination of an anion deficient oxide.[21] The first clear point for these and many other related materials is the strong preference for fluoride to occupy the apical position in the rocksalt/fluorite layers. In the shown examples this causes complete oxide/fluoride ordering, while K_2NbO_3F[17] and Ba_2ScO_3F[16] have a mixture of oxide and fluoride on apical sites (though only oxide on the equatorial site). A further possibility is for fluoride to occupy an interstitial site with expansion of this layer, this has been observed commonly in phases produced by fluorination. This is observed in $Sr_2CuO_2F_{2+\delta}$[1] and $La_{1.9}Sr_{1.1}Cu_2O_5F_2$.[21] In the anion rich $La_{1.2}Sr_{1.8}Mn_2O_7F_2$ all the fluoride is found in such an interstitial site and the apical sites of manganese contain only oxide ions.[21] In $Sr_3Fe_2O_6F_{0.87}$ all the fluoride is accounted for by those contained in the apical site at iron and there is no evidence of further fluoride in the structure. The *c*-axis expansion observed in $Sr_3Fe_2O_6F_{0.87}$ is also considerably less than that typically observed when this interstitial site is occupied (*e.g.* a 1.4 Å expansion is observed on fluorination of $La_{1.9}Sr_{1.1}Cu_2O_6$). However this type of interstitial site could be involved in the process of fluoride insertion. Fluoride ions could possibly enter the interstitial site and then cause the rearrangement as they move into the apical site at iron.

Sr_2FeO_3F was originally reported by Galasso and Darby[17] as being isostructural with K_2NbO_3F with a tetragonal K_2NiF_4 or T structure type. On the basis of thermal expansion measurements and consideration of the *c*/*a* ratios the fluoride anions in Sr_2FeO_3F and K_2NbO_3F were assigned to the apical sites of the B cation coordination octahedron. This site was therefore assumed to be an equal mixture of oxide and fluoride. Further studies[18,32] showed that the samples produced by Galasso and Darby[17] were slightly oxidised but that pure iron(III) samples can be obtained with confirmation by ^{57}Fe Mössbauer studies. It was also shown, however, that there were weak reflections in the PXD patterns which could not be indexed with the *I*4/*mmm* space group indicating that the iron environment described by *I*4/*mmm* is probably wrong. The Mössbauer spectra were consistent with a highly distorted octahedral iron(III) environment. Structural characterisation of Sr_2FeO_3F using the coordinate description of Ba_2InO_3F proved much more satisfactory. The supercell reflections are then successfully modelled and the iron coordination provides an explanation for the asymmetry indicated in the Mössbauer spectrum. It is clear that Sr_2FeO_3F and K_2NbO_3F are not isostructural. The bond valence calculations confirmed that Sr_2FeO_3F exhibits the same anion ordering as was observed in Ba_2InO_3F,[16] a reexamination of K_2NbO_3F has shown that the same ordering does not occur in this phase.[33] The two structures are shown for comparison in Fig. 8.

The *c*/*a* ratio of Sr_2FeO_3F from this study was 3.41, in close agreement with the earlier work. The *c*/*a* ratios of Sr_2FeO_3F, K_2NbO_3F (3.46) and Ba_2InO_3F (3.36) do not differ greatly, but there is a marked difference in the *c*-axis thermal expansion coefficients where these have been measured. The rate of expansion in this direction is 1.3 times that of the *a* direction in Sr_2FeO_3F but twice that in the *a* direction in K_2NbO_3F, perhaps indicative of the change in structure. This parameter has not been measured for Ba_2InO_3F or for Ba_2ScO_3F, which is isostructural with K_2NbO_3F.

The PND refinement of the fluorination product of Ba_2InFeO_5 suggests a composition $Ba_2InFeX_{5.68}$. Assuming no displacement of oxide the composition is $Ba_2InFeO_5F_{0.68}$ and the sample would contain 2.4% fluoride and 34% iron(V). The fluoride analysis suggests 2.7% fluoride and the Mössbauer 30% iron(V). A composition $Ba_2InFeO_{4.92}F_{0.76}$ would exactly match both these results but the difference is too small to reliably infer that any oxide displacement has occurred.

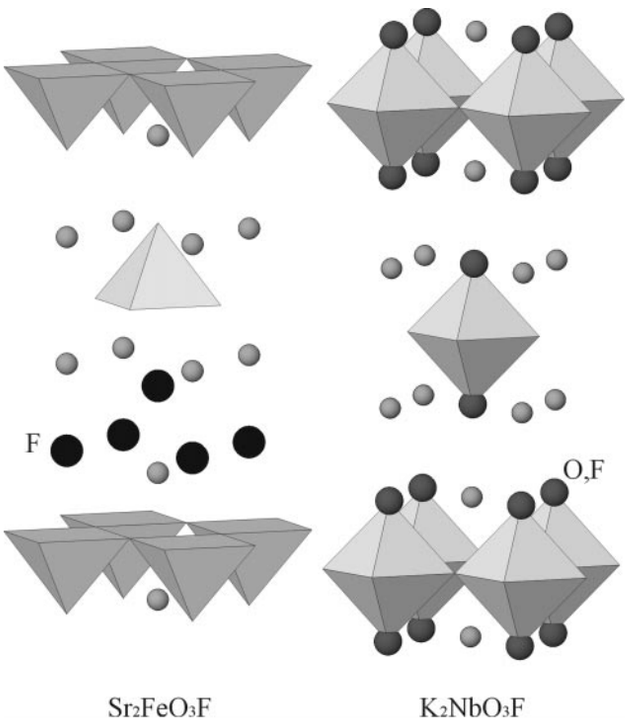

Fig. 8 Structures of Sr_2FeO_3F and K_2NbO_3F.

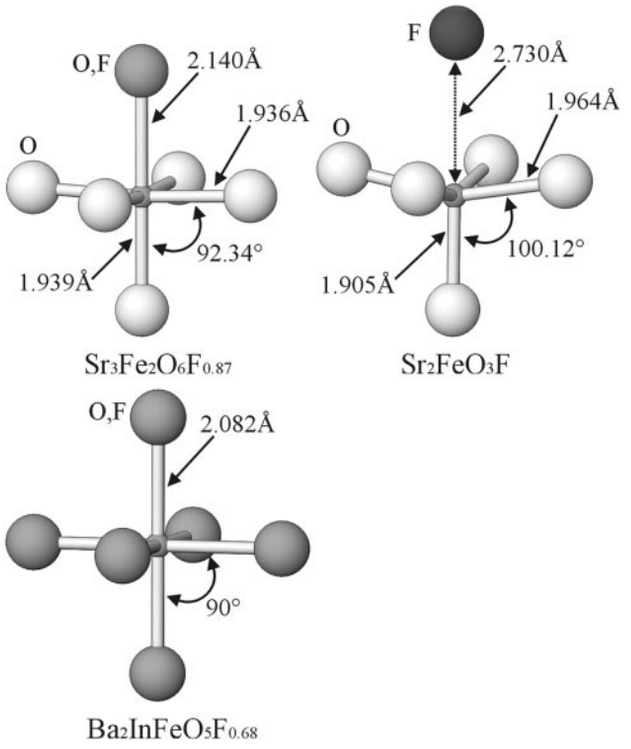

Fig. 9 Iron coordination spheres.

The iron coordination spheres of the three phases studied are shown in Fig. 9. In $Sr_3Fe_2O_6F_{0.87}$ the iron–oxygen distances are similar to those observed in the $Sr_3Fe_2O_{7-x}$ system (equatorial 1.98–1.93 Å, apical 1.89–1.94 Å). The Fe–(O,F) distances are elongated and the O–Fe–O bond angles are $>90°$, reflecting the tendency of fluoride in these structures to coordinate weakly, if at all, to the B-cation.[1,16] The square based pyramid of oxygens around iron of Sr_2FeO_3F is virtually identical to that observed in $Sr_3Fe_2O_6$ (equatorial 1.98 Å, apical 1.89 Å, O–Fe–O 100.44°). This reflects the non-bonding nature of this fluoride with respect to iron. In $Ba_2InFeO_5F_x$ the coordination sphere is completely regular with Fe–O bond lengths which are greater than those observed in the other phases because the B-cation site is shared by indium, which is considerably larger ($r_{In^{3+}} = 0.80$ Å[34]) than iron ($r_{Fe^{3+/4+}} = 0.55$–0.60 Å).

Conclusions

The reactions of $Sr_3Fe_2O_6$ and Ba_2InFeO_5 with elemental fluorine result in mixed valent iron(III)/iron(V) oxyfluoride materials. $Sr_3Fe_2O_6F_{0.87}$ is a Ruddlesden–Popper type material with a disordered mixture of oxide and fluoride ions located in the rocksalt layer. This location of the fluoride ions requires a structural rearrangement, with oxide ions moving into the perovskite bilayer. $Ba_2InFeO_5F_{0.68}$ is a defect cubic perovskite with a disordered oxide/fluoride distribution. The K_2NiF_4 type material Sr_2FeO_3F has anion ordering such that alternate rocksalt layers contain oxide or fluoride, not a mixture as previously described, resulting in square based pyramidal FeO_5 coordination to iron.

Acknowledgements

This work was carried out with support from the EPSRC under grant GR/K55578 (A.L.H.) and a studentship (G.S.C.) and from the University of Southampton through a partial studentship (R.L.N.).

References

1 M. Al-Mamouri, P. P. Edwards, C. Greaves and M. Slaski, *Nature (London)*, 1994, **369**, 382.
2 J. B. McChesney, R. C. Sherwood and J. F. Potter, *J. Chem. Phys.*, 1965, **43**, 1908.
3 Y. Takeda, S. Naka, M. Takano, T. Takada and M. Shimada, *Bull. Inst. Chem. Res. Jpn.*, 1978, **13**, 61.
4 Y. Takeda, Y. Yamaguchi, H. Takei and H. Wattanabe, *J. Solid State Chem.*, 1977, **42**, 101.
5 S. E. Dann, D. B. Currie, M. T. Weller, M. F. Thomas and A. D. Al-Rawas, *J. Solid State Chem.*, 1994, **109**, 134.
6 J. G. Bednorz and K. A. Müller, *Z. Phys. B*, 1986, **64**, 189.
7 S. N. Ruddlesden and P. Popper, *Acta Crystallogr.*, 1957, **10**, 538; 1958, **11**, 54.
8 S. E. Dann, D. B. Currie and M. T. Weller, *J. Solid State Chem.*, 1991, **92**, 237.
9 S. E. Dann, D. B. Currie and M. T. Weller, *J. Solid State Chem.*, 1992, **97**, 179.
10 S. E. Dann, M. T. Weller, D. B. Currie, M. F. Thomas and A. D. Al-Rawwas, *J. Mater. Chem.*, 1993, **3**, 1231.
11 R. L. Needs and M. T. Weller, *J. Solid State Chem.*, 1998, **139**, 422.
12 W. Rüdorff and D. Krug, *Z. Anorg. Allg. Chem.*, 1964, **329**, 211.
13 B. L. Chamberland, *Mater. Res. Bull.*, 1971, **6**, 311.
14 G. Demazeau, J. Grannec, A. Marbeuf, J. Poiter and P. Hagenmuller, *C. R. Hebd. Seances Acad. Sci., Ser. C*, 1969, **269**, 987.
15 B. L. Chamberland, ch. 4 in *Inorganic Solid Fluorides: Chemistry and Physics*, ed. P. Hagenmuller, Materials Science and Technology series, Academic Press, Orlando, FL, 1985.
16 R. L. Needs, M. T. Weller, U. Scheler and R. K. Harris, *J. Mater. Chem.*, 1996, **6**, 1219.
17 F. Galasso and W. Darby, *J. Phys. Chem.*, 1962, **66**, 1318.
18 F. Menil, N. Kinomura, L. Fournes, J. Poitier and P. Hagenmuller, *Phys. Status Solidi A*, 1981, **64**, 261.
19 G. Le Flem, R. Colmet, C. Chaumont, J. Claverie and P. Hagenmuller, *Mater. Res. Bull.*, 1976, **11**, 389.
20 R. L. Needs and M. T. Weller, *J. Chem. Soc., Dalton Trans.*, 1995, 3015.
21 C. Greaves, J. L. Kissick, M. G. Francesconi, L. D. Aikens and L. J. Gillie, *J. Mater. Chem.*, 1999, **9**, 111.
22 C. S. Knee and M. T. Weller, personal communication. Synthesis was carried out by reaction of the component oxides in a vacuum sealed silica tube lined with an alumina crucible at 1000 °C for two days.
23 Powder Diffraction File, Release 1998, International Centre for Diffraction Data, Swarthmore, PA 19073-3273, USA.
24 C. Larson and R. B. Von Dreele, *GSAS Generalised Structure Analysis System*, MS-H805, Los Alamos, NM, 1990.
25 G. J. Long, T. E. Cranshaw and G. Longworth, *Mössbauer Effect Ref. Data J.*, 1983, **6**, 42.
26 R. Greenhalgh and J. R. Riley, *Anal. Chim. Acta*, 1961, **25**, 179.
27 L. Köster, H. Rauch and E. Seymann, *At. Data Nucl. Tables*, 1991, **49**, 65.
28 F. Galasso and W. Darby, *J. Phys. Chem.*, 1963, **67**, 1451.
29 *Physica C—Crystal Structures of the High-T_c Superconducting Copper Oxides*, ed. H. Shaked, P. M. Keane, J. C. Rodriguez, F. F. Owen, R. L. Hitterman and J. D. Jorgensen, Elsevier, Amsterdam, 1994.
30 R. L. Needs, M. F. Thomas and M. T. Weller, in preparation.
31 (*a*) D. Brown and D. Altermatt, *Acta Crystallogr., Sect. B*, 1985, **41**, 244; N. E. Brese and M. O'Keefe, *Acta Crystallogr., Sect. B*, 1991, **47**, 192; (*b*) W. A. Dollase, *J. Appl. Crystallogr.*, 1986, **19**, 267; A. March, *Z. Kristallogr.*, 1932, **81**, 285.
32 L. Fournes, N. Kinomura and F. Menil, *C. R. Acad. Sci., Ser. C*, 1980, **291**, 235.
33 R. L. Needs, Ph.D. thesis, University of Southampton, 1997.
34 R. D. Shannon, *Acta Crystallogr., Sect. A*, 1976, **32**, 751.

Paper 9/05730G